Organic Electronics 10 (2009) 1109–1115

Contents lists available at ScienceDirect

Organic Electronics

journal homepage: www.elsevier.com/locate/orgel

Efficient bulk heterojunction solar cells based on a low-bandgap polyfluorene copolymers and fullerene derivatives

Jen-Hsien Huang [a], Kuang-Chieh Li [c], Hung-Yu Wei [b], Po-Yen Chen [a], Lu-Yin Lin [a], Dhananjay Kekuda [d], Hong-Cheu Lin [c], Kuo-Chuan Ho [a,b], Chih-Wei Chu [d,e,*]

[a] Department of Chemical Engineering, National Taiwan University, Taipei, Taiwan
[b] Institute of Polymer Science and Engineering, National Taiwan University, Taipei, Taiwan
[c] Department of Materials Science and Engineering, National Chiao Tung University, Hsinchu, Taiwan
[d] Research Center for Applied Sciences, Academia Sinica, Taipei, Taiwan
[e] Department of Photonics National Chiao Tung University, Hsinchu, Taiwan

ARTICLE INFO

Article history:
Received 4 May 2009
Received in revised form 28 May 2009
Accepted 28 May 2009
Available online 6 June 2009

PACS:
73.50.Pz
73.61.Ph

Keywords:
Polymer solar cell
Polyfluorene
Phenothiazine derivative
Narrow bandgap polymers
Bulk heterojunction

ABSTRACT

A low-bandgap polymer (PF-PThCVPTZ) consisted of fluorene and phenothiazine was designed and synthesized. With the donor–acceptor segment, the partial charge transfer can be built in the polymer backbone leading to a wide absorbance. The absorption spectrum of PF-PThCVPTZ exhibits a peak at 510 nm and an absorption onset at 645 nm in the visible range. As blended with [6,6]-phenyl-C61-butyric acid methyl ester (PCBM) as an electron acceptor, narrow bandgap PF-PThCVPTZ as electron donor shows significant solar cell performance. Under AM 1.5 G, 100 mA/cm^2 illumination, a power conversion efficiency (PCE) of 1.85% was recorded, with a short circuit current (J_{SC}) of 5.37 mA/cm^2, an open circuit voltage (V_{OC}) of 0.80 V, and a fill factor (FF) of 43.0%.

1. Introduction

Harvesting energy directly from sunlight using photovoltaic cells is a very important way to utilize renewable energy of the nature, especially for the development of organic solar cells. Compared with inorganics, organic materials provide unlimited potential to modify the chemical structure achieving a better opto-electronic characteristic via organic chemistry which allows the devices revealing better performance. Recently, dye-sensitized solar cells based on nanoporous TiO_2 thin film can reach an efficiency as high as 10%. However, the requirement of liquid electrolytes and elevated annealing temperature in dye-sensitized solar cells are still a very challenging issue to be overcome for commercial applications. Much research has been focused on development of bulk heterojunction (BHJ) solar cells to resolve the drawback. BHJ solar cells have attracted a great deal of interest recently due to their potential for low-cost, large area, light weight and flexible photovoltaic (PV) devices. The main feature of BHJ solar cells is the significantly increased in the interface between the donor and acceptor allowing an efficient charge separation compared to the planar interface of bilayer cells leading to a larger photocurrent.

* Corresponding author. Address: Research Center for Applied Sciences, Academia Sinica, Taipei, Taiwan. Tel.: +886 2 27898000x70; fax: +886 2 27826680.
E-mail address: gchu@gate.sinica.edu.tw (C.-W. Chu).

1566-1199/$ - see front matter © 2009 Elsevier B.V. All rights reserved.
doi:10.1016/j.orgel.2009.05.025

Until now, PCE up to 5% has been achieved from the BHJ of poly(3-hexylthiophene) (P3HT) blended with PCBM [1]. Although the transport properties have been dramatically improved by vertical phase separation of both donor and acceptor due to the self-organization effect [2–5], they still lack the absorption in the red and infrared regions. Therefore, great deal efforts have been undertaken to enhance the J_{SC} of solar cells by enhancing the absorption spectra of active layers. Recently, much work has been focused on synthesis the conjugated polymers [6–13]. Among several types of organics materials, polymer with electron donor–acceptor architectures is one of the most efficient ways to synthesize the narrow bandgap polymers. The effect of intramolecular charge transfer between the electron donor and acceptor units has been found in the polymers with donor–acceptor architectures leading to a narrow bandgap [14–21].

Recently, much BHJ polymer solar cells using polyfluorene based alternating copolymers as donor have been reported due to their high charge carrier mobility [22,17]. However, polyfluorene copolymers in general have high bandgaps giving blue-shift optical absorption and hence have limited the photocurrent generation. For example, poly[9,9'-dioctyl-fluorene-co-bithiophene] (F8T2) only absorbs light at wavelengths less than 500 nm [23]. Even though F8T2 exhibits excellent thermo tropic liquid crystallinity allowing better chain packing via self-assembly [24], the poor absorption still depresses the extraction of photocurrent dramatically. In this article, the BHJ device performance of a low-bandgap polyfluorene copolymer which comprises the phenothiazine units is reported. The copolymer used for here is referred to as PF-PThCVPTZ. With the incorporation of phenothiazine units into PF, the absorption can be stretched due to the donor–acceptor structure.

2. Experimental

2.1. Synthetic procedures

2.1.1. Synthesis

Monomer was synthesized according to a reported procedure [25], and the characterization is described as follows. The copolymer PF-PThCVPTZ is shown in Scheme 1, and this synthetic procedure is described as follows.

2.1.2. Monomer

Yield: 53%. ^{1}H NMR ($CDCl_3$, ppm), δ: 7.72 (dd, J = 8.7, 1.8 Hz, 1H), 7.45–7.36 (m, 3H), 7.29–7.18 (m, 3H), 7.07–7.01 (m, 5H), 6.79 (d, J = 8.7 Hz, 2H), 3.80 (t, J = 7.2 Hz, 2H), 1.80 (m, 2H), 1.45–1.14 (m, 6H), 0.89 (m, 3H). ^{13}C NMR ($CDCl_3$, ppm), δ: 148.11, 146.00, 143.66, 140.67, 140.14, 138.08, 135.80, 134.54, 132.05, 131.00, 130.89, 130.67, 128.54, 128.11, 127.49, 126.56, 125.31, 124.32, 123.88, 123.53, 122.87, 116.56, 116.49, 115.43, 114.99, 112.64, 112.62, 102.51, 100.94, 48.00, 31.35, 29.67, 26.49, 22.59, 13.98. MS (EI): m/z [M^+] 788.94, calcd m/z [M^+] 789.0. Anal. Calcd for $C_{36}H_{27}Br_2N_3S_4$: C, 54.75; H, 3.45; N, 5.32. Found: C, 55.19; H, 3.90; N, 4.82.

2.1.3. General procedure for the synthesis of PF-PThCVPTZ

The synthetic route of polymers is shown in Scheme 1. The polymerizations was carried out through the palladium(0)-catalyzed Suzuki coupling reactions. Into 50 mL of two-neck flask, 1 equiv of monomer and 1 equiv of 2,7-bis-(4,4,5,5-tetramethyl-1,3,2-dioxaborolan-2-yl)-9,9-

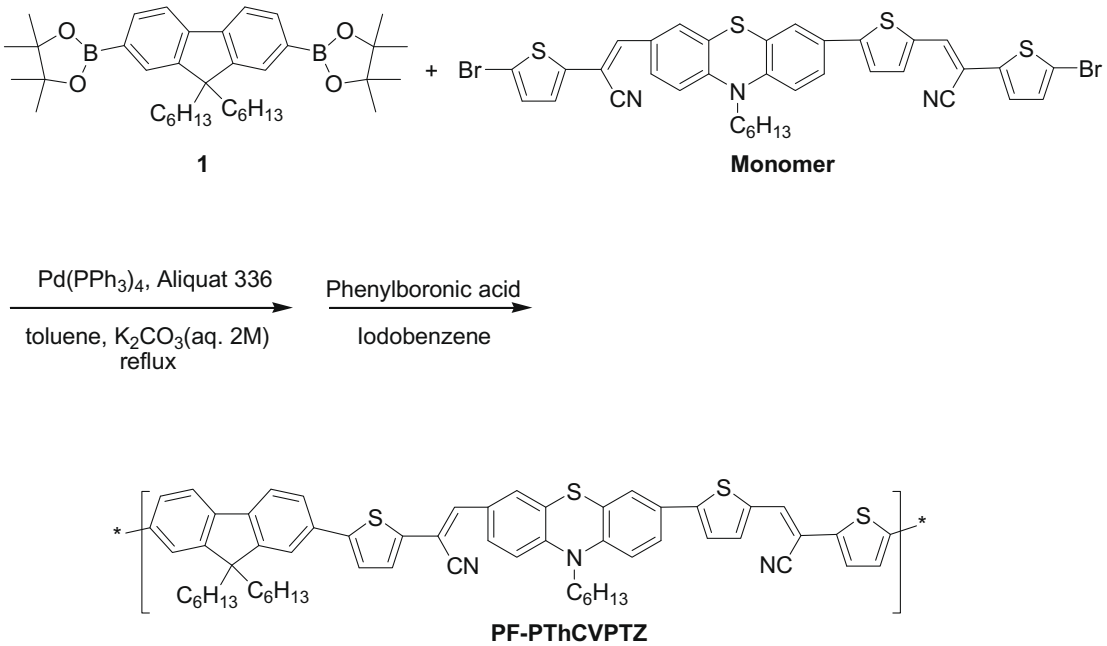

Scheme 1. Synthetic routes of PF-PThCVPTZ.

dihexylfluorene (1) were added in 10 mL of anhydrous toluene. The Pd(0) complex, Pd{P(*p*-tolyl)$_3$}$_3$ (1 mol%), was transferred into the mixture in a dry environment. Then, 2 M aqueous potassium carbonate and the phase transfer catalyst, i.e., aliquat 336 (several drops), were subsequently transferred via cannula into the previous mixture under nitrogen. The reaction mixture was stirred at 90 °C for 2 days, and then the excess amount of iodobenzene and phenylboronic acid, the end-capper, dissolved in 1 mL of anhydrous toluene was added and stirring for 4 h, respectively. The reaction mixture was cooled to 50 °C and added slowly into a vigorously stirred mixture of 300 mL of methanol. The polymers were collected by filtration and reprecipitation from methanol. The crude polymers were further purified by washing with acetone for 3 days in a Soxhlet apparatus to remove oligomers and catalyst residues. The resulting polymers were soluble in common organic solvents.

2.2. Fabrication of photovoltaic devices

The PV devices in this study consists of a layer of PF-PThCVPTZ:PCBM blend thin film sandwiched between transparent anode indium tin oxide (ITO) and metal cathode. Before device fabrication, the ITO glasses (1.5×1.5 cm^2) were ultrasonically cleaned in detergent, de-ionized water, acetone and isopropyl alcohol before the deposition. After routine solvent cleaning, the substrates were treated with UV ozone for 15 min. Then, a modified ITO surface was obtained by spin-coating a layer of poly(ethylene dioxythiophene): polystyrenesulfonate (PEDOT:PSS) (~30 nm). After baking at 130 °C for 1 h, the substrates were then transferred into a nitrogen-filled glove box. The polymer PV devices were fabricated by spin-coating blend of PF-PThCVPTZ:PCBM on the PEDOT:PSS modified ITO surface. Subsequently, a 30 and 100 nm thick of calcium and aluminum was thermally evaporated under vacuum at a pressure below 6×10^{-6} Torr through a shadow mask. The active area of the device was 0.12 cm^2. In the hole-only devices, the MoO_3 was used to replace Ca with higher work function ($\Phi = 5.3$ eV), which is a good hole injection contact for PF-PThCVPTZ:PCBM [26]. The MoO_3 was thermally evaporated with a thickness of 20 nm and then capped with 50 nm of Al. For the electron-only devices, PEDOT:PSS layer was replaced with $CsCO_3$ ($\Phi = 2.9$ eV) which has been used as an efficient electron injection layer [27]. The Cs_2CO_3 was thermally evaporated with a thickness of 2 nm. The active layers were annealed at 130 °C for 20 min before the hole and electron-only devices were fabricated.

2.3. Characterization of polymer films and PV devices

Cyclic voltammetry (CV) studies were performed with a three-electrode cell with 0.1 M $LiClO_4$/ACN using ITO as the working electrode, a platinum sheet as the counter electrode, and nonaqueous Ag/Ag$^+$ (containing 0.01 M $AgNO_3$ and 0.1 M $TBAClO_4$ in ACN) as the reference electrode. For measuring absorption and photoluminescence (PL) emission properties of polymer films, samples were fabricated on a glass substrate. The UV–visible absorption spectra were measured using a Jasco-V-670 UV–visible spectrophotometer. PL spectra were obtained using a Hitachi F-4500 photoluminescence. Surface morphologies were observed by an atomic force microscopy (AFM, Digital instrument NS 3a controller with D3100 stage). The thickness of all polymer films was measured using a surface profiler (Alpha-step IQ, KLA Tencor). Current–voltage (*J*–*V*) characteristics were measured in the glove box under nitrogen atmosphere with simulated AM 1.5 G irradiation at 100 mW/cm^2 using a xenon lamp based solar simulator (Thermal Oriel 1000 W). The light intensity was calibrated by a mono-silicon photodiode with KG-5 color filter (Hamamatsu, Inc.). The external quantum efficiency (EQE) action spectrum was obtained at short-circuit condition. The light source was a 450 W Xe lamp (Oriel Instrument, model 6266) equipped with a water-based IR filter (Oriel Instrument, model 6123NS). The light output from the monochromator (Oriel Instrument, model 74100) was focused onto the photovoltaic cell under test.

3. Results and discussion

The CV was performed to investigate the electronic state of the PF-PThCVPTZ. As shown in Fig. 1a, the CV of PF-PThCVPTZ presents an oxidation process ($E_{ox}^{1/2} = 0.89$ V vs. Ag/Ag$^+$) and a reduction process ($E_{red}^{1/2} = -1.08$ V). Furthermore, the E_{ox}^{onset} and E_{red}^{onset} are 0.78 and −0.81 V, respectively, which allows us to calculate the highest molecular orbital (HOMO) and lowest molecular orbital (LUMO) according to following equation [28]: $E_{HOMO/LUMO} = [-(E_{onset} - 0.45) - 4.8]$ eV. The factor of 0.45 and 4.8 are derived from the formal potential for ferrocene vs. Ag/Ag$^+$ and the energy level of ferrocene below the vaccum. On the basis of these electrochemical data, the HOMO and LUMO levels can be defined as −5.13 and −3.54 eV. Therefore, the bandgap offset between the LUMOs of PF-PThCVPTZ and PCBM is enough for electrons to be driven forward. Moreover, the polymer also reveals a multiply

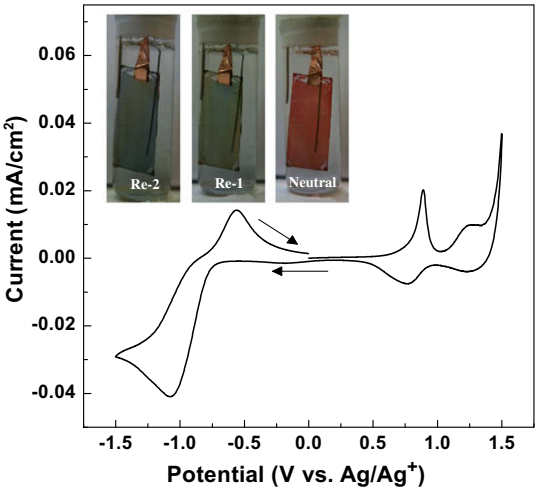

Fig. 1. Cyclic voltammogram of PF-PThCVPTZ film cast on a platinum wire in 0.1 M $LiClO_4$/acetonitrile at 50 mV/s. (Inset: picture of the polymer film on the ITO electrode at different coloration states.)

colored electrochromic property. Fig. 1a shows the photographs of PF-PThCVPTZ films in uncharged (neutral, red), half (Re-1, green) and full (Re-2, blue) reduction states. The film colors are homogenerously distributed across the electrode surface and the color changes are easily detected by the naked eye.

The normalized optical absorption spectra of the PF-PThCVPTZ in solution and solid film and PL emission spectra of pristine polymer and their blend films with PCBM are depicted in Fig. 2. The solid film shows similar absorption pattern compared with the one of solution. However, slight red-shift still can be observed due to the interchain association and aggregation in the solid state. The PF-PThCVPTZ film reveals a spectral absorption with a peak at 510 nm and an absorption onset at 645 nm. Furthermore, the corresponding PL emission maxima λ_{em} of PF-PThCVPTZ is centered at 660 nm. The PL emission is significantly quenched by the addition of 50 wt% PCBM. This highly efficient photoluminescence quenching is the consequence of ultrafast photoinduced charge transfer from the polymer to PCBM. Based on these characterizations, the copolymer is an excellent candidate to fabricate the photovoltaic devices.

The current density for the devices with varying active layer thickness are plotted in Fig. 3. The devices were fabricated by spin coating a solution of PF-PThCVPTZ/PCBM (1:1 in weight, 4 mg/mL) dissolved in 1,2-dichlorobenzene (DCB). The V_{OC} remains unchanged at about 0.8 V on changing the active layer thickness as shown in the inset. However, the J_{SC} and the PCE of the devices vary significantly with thickness. The J_{SC} varies from as low as 1.20 mA/cm^2 (for the device with active layer thickness,

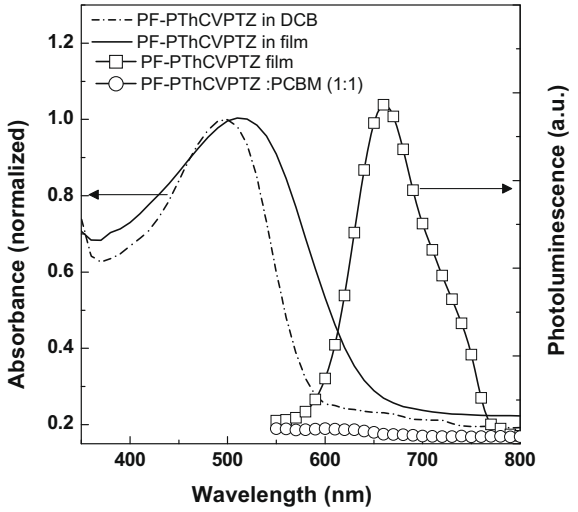

Fig. 2. UV–vis spectrum in DCB (dash line) and in the solid state (solid line), photoluminescence in solid state (□) and photoluminescence quenching for PF-PThCVPTZ:PCBM (1:1) (○).

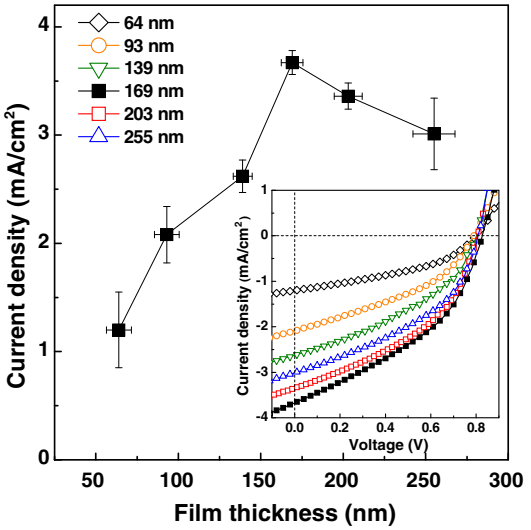

Fig. 3. J_{SC} plotted as a function of the thickness of active layer for the PF-PThCVPTZ:PCBM solar cells. (Inset: corresponding *J–V* characteristics.)

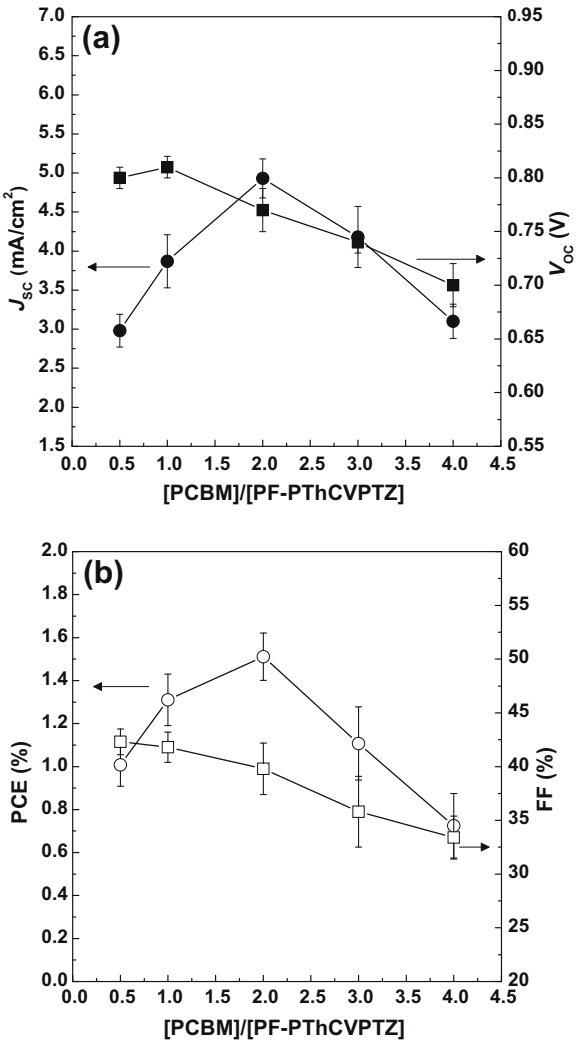

Fig. 4. J_{SC}, V_{OC}, FF and PCE plotted as a function of the composition for the PF-PThCVPTZ:PCBM solar cells.

t = 64 nm) to as high as 3.67 mA/cm^2 (t = 170 nm) and back to 3.0 mA/cm^2 (t = 255 nm). The increased J_{SC} is contributed from the larger absorbance with thicker active layer. However, the J_{SC} decreases with a thickness larger than 169 nm due to the large series resistance and poor charge transport leading to a serious recombination [29]. An efficiency of 1.23% is achieved for the device with t = 170 nm.

Fig. 4 shows the performance parameters of the measured devices, namely J_{SC}, V_{OC}, FF and PCE as a function of PCBM weight ratios. First, the J_{SC} increases from 2.98 for the device with containing 33 wt% PCBM to 3.87, and 4.93 mA/cm^2 for those containing 50 and 66 wt% PCBM. However, the J_{SC} decreases with a larger PCBM weight ratio as shown in Fig. 3a which means that a higher PCBM weight ratio leads to an imbalanced mobility between donor and acceptor, thus impeding the charge transport. Second, the V_{OC} and the FF strongly decrease with PCBM loading, resulting in a doubling of the calculated PCE when increasing the PCBM concentration from 33 to 80 wt%. According to our previous work [30], we have found that the values for V_{OC} and FF based on polyfluorene copolymer decrease monotonically with increasing fullerene content in the BHJ films. This can be rationalized by the incomplete charge generation and transport resulted from the aggregation of the large amount of fullerenes [31]. The best cell has an active layer thickness of about 180 nm, containing 66 wt% of PCBM with a J_{SC} of 4.93 mA/cm^2, a V_{OC} of 0.77 V, a FF of 40%, and a PCE of 1.51%.

In order to control the morphology of the blending films, we investigated the effect of solvents with different boiling points. Fig. 5 compares the morphology of the films cast from chloroform (CF), chlorobenzene (CB), DCB and 1,2,4-trichlorobenzene (TCB) with the boiling points of 60, 132, 180 and 218 °C, respectively. The images are obtained in tapping mode for a 2 × 2 μm^2 surface area. It can be found the films spin-cast from CB, DCB and TCB show a coarse chainlike feature stretching across the surfaces. With higher boiling point, the chainlike feature is more obvious and the root mean square roughness (RMS) also increases from 4.3 (for the film cast from CB) to 7.8 (TCB). These chainlike features are originated from the strong π–π stacking of the polymer chains which is believed to enhance the charge transport [32,33]. This feature

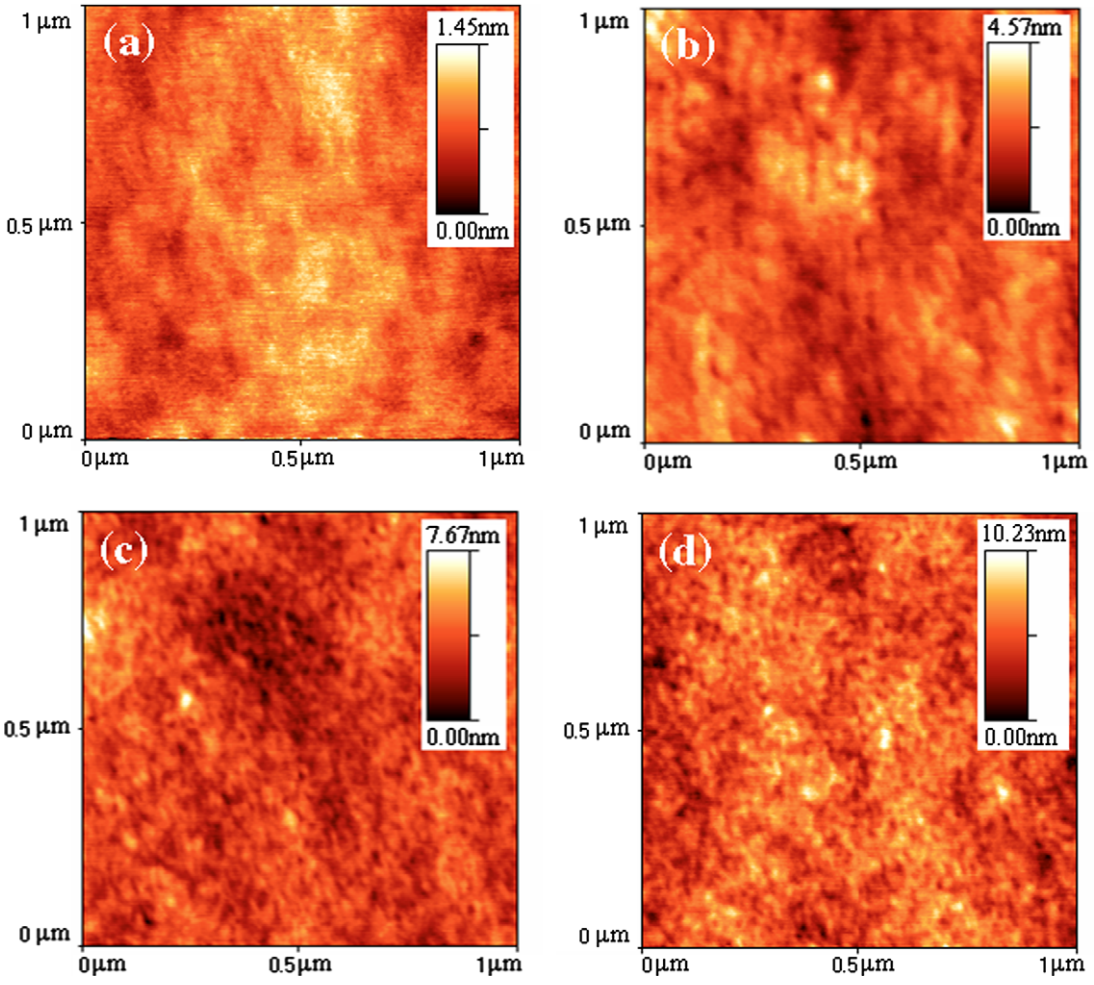

Fig. 5. AFM images of the blended films cast from (a) CF, (b) CB, (c) DCB and (d) TCB.

is well known and easily reproducible for the P3HT:PCBM blends using slow growth with high boiling point solvent such as TCB or DCB. In contrast, the film prepared from CF solution appears a very smooth surface without apparent nanostructure. Although CF is a good solvent for PF-PThCVPTZ, however, its low boiling point and rapid evaporation limit the time for crystallization during the spin-coating process.

To further understand the dependence of charge transfer properties on morphologies that were introduced by varying the solvents, we have performed dark current measurements on hole-only and electron-only devices based on the blend films. The charge mobilities were calculated by space-charge limited current (SCLC) [34]. The dark current is given by $J = 9\varepsilon_0\varepsilon_r\mu V2/8L^3$, where $\varepsilon_0\varepsilon_r$ is the permittivity of the polymer, μ is the carrier mobility, and L is the device thickness. The hole and electron mobilities of the blend films preapard from different solvents are summarized in Table 1. For the device made by CF have the lowest hole and electron mobility. Overall, the largest mobility can be found in the devices fabricated from TCB. The hole and electron mobility up to 1.93×10^{-8} and 2.41×10^{-8} $m^2 V^{-1} s^{-1}$ is observed. Furthermore, we observed more balanced charge mobility ($\mu_h/\mu_e = 0.8$) in the film cast from TCB which can enhance the photocurrent.[35,36] For both DCB and TCB (which has a higher boiling point) it takes 10–15 min for the film to dry, while films cast from CF would dry within a few seconds of spinning. Therefore, the molecules in TCB can self-organization over a long time to form a thermodynamically favored structure leading to higher charge mobility [37,38].

Fig. 6 shows the J–V curves and EQE of the PV devices fabricated from various solvents. The J_{SC} values of the devices fabricated from CF, CB, DCB and TCB are 2.45, 3.58, 4.73 and 5.37 mA/cm^{-2}, and the FF values are 45.4, 41.4, 38.3 and 43.0%, respectively. The V_{OC} values of all cases are almost the same (0.80 V). As a result, the PCE of 1.84% is the highest among these devices which is obtained from TCB. The highest J_{SC} of device fabricated from TCB can be realized by the slow growth effect which provides a charge transport channel formed from self-organization leading to a higher photocurrent. This is supported by EQE characterization. After measuring the J–V curves, the devices were encapsulated in a nitrogen-filled glove box, and the EQE of the devices were measured in air. As shown in the inset, the devices exhibit a photoresponse covering from 350 to 650 nm. It can be seen that the EQE values increase by using solvents with higher boiling points. These results are in good agreement with the values of J_{SC}. The EQE for the device fabricated from CF shows a maximum of 20.7% at a wavelength of 370 nm. On the other hand, for the device fabricated from TCB, the EQE maximum increases to 39.8 at 450 nm leading to a larger J_{SC}.

Table 1
A summary of the charge mobility for the PF-PThCVPTZ:PCBM films cast from different solvents.

Solvent	Boiling point (°C)	Thickness (nm)	μ_h ($m^2 V^{-1}s^{-1}$)	μ_e ($m^2 V^{-1}s^{-1}$)	μ_h/μ_e
CF	60	178 ± 2	8.07×10^{-9}	1.39×10^{-8}	0.58
CB	132	172 ± 3	1.18×10^{-8}	1.91×10^{-8}	0.62
DCB	180	168 ± 2	1.74×10^{-8}	2.24×10^{-8}	0.78
TCB	218	171 ± 1	1.93×10^{-8}	2.41×10^{-8}	0.80

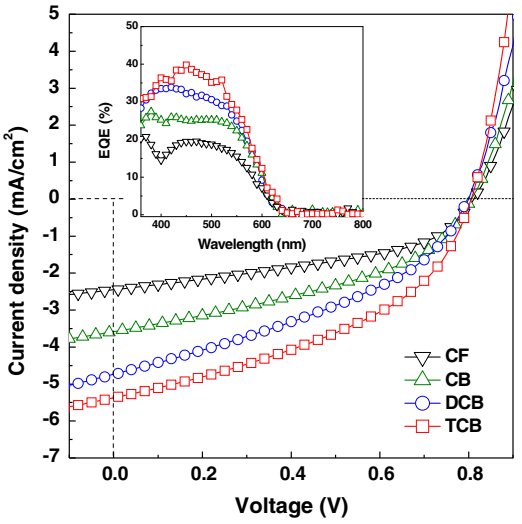

Fig. 6. J–V curves of the PF-PThCVPTZ:PCBM solar cells fabricated from different solvents. (Inset: corresponding EQE characteristics.)

4. Conclusion

An alternating PF copolymer, PF-PThCVPTZ, containing a low-bandgap donor–acceptor segment has been designed and synthesized for use in PV devices. A broad absorption spectrum in PF-PThCVPTZ film covers the visible solar spectrum, resulting in an extended photocurrent response. Under AM 1.5 G 100 mA/cm^2 illumination, the devices fabricated from TCB with 67 wt% PCBM reveal a PCE of 1.84%. Based on these findings, PF-PThCVPTZ is a potential candidate for application in polymer solar cells.

Acknowledgements

The authors are also grateful to the National Science Council (NSC), Taiwan, (NSC 96-2221-E-001-017-MY2 and NSC 96-2628-E-007-030-MY2) and Academia Sinica, Taiwan for financial support.

References

[1] J.Y. Kim, S.H. Kim, H.H. Lee, K. Lee, W. Ma, X. Gong, A.J. Heeger, Adv. Mater. 18 (2006) 572.
[2] G. Li, V. Shrotriya, J. Huang, Y. Yao, T. Moriarty, K. Emery, Y. Yang, Nat. Mater. 4 (2005) 864.
[3] M. Campoy-Quiles, T. Ferenczi, T. Agostinelli, P.G. Etchegoin, Y. Kim, T.D. Anthopoulos, P.N. Stavrinou, D.D.C. Bradley, J. Nelson, Nat. Mater. 7 (2008) 158.
[4] G. Li, Y. Yao, H. Yang, V. Shrotriya, G. Yang, Y. Yang, Adv. Funct. Mater. 17 (2007) 1636.
[5] S.S. van Bavel, E. Sourty, G. de With, J. Loos, Nano Lett 9 (2009) 507.
[6] A. Gadisa, W. Mammo, L.M. Andersson, S. Admassia, F. Zhang, M.R. Andersson, O. Inganäs, Adv. Funct. Mater. 17 (2007) 3836.
[7] P.T. Boudreault, A. Michaud, M. Leclerc, Macromol. Rapid Commun. 28 (2007) 2176.
[8] N. Blouin, A. Michaud, D. Gendron, S. Wakim, E. Blair, R.N. Plesu, M. Belletête, G. Durocher, Y. Tao, M. Leclerc, J. Am. Chem. Soc. 130 (2008) 732.
[9] Y. Li, Y. Zou, Adv. Mater. 20 (2008) 2952.

[10] Y. Liang, Y. Wu, D. Feng, S.T. Tsai, H.J. Son, G. Li, L. Yu, J. Am. Chem. Soc. 131 (2009) 56.
[11] J. Hou, H.Y. Chen, S. Zhang, G. Li, Y. Yang, J. Am. Chem. Soc. 130 (2008) 16144.
[12] W.Y. Wong, X.Z. Wang, Z. He, K.K. Chan, A.B. Djurišic, K.Y. Cheung, C.T. Yip, A.M.C. Ng, Y.Y. Xi, C.S.K. Mak, W.K. Chan, J. Am. Chem. Soc. 129 (2007) 14372.
[13] J. Hou, T.L. Chen, S. Zhang, H.Y. Chen, Y. Yang, J. Phys. Chem. C 113 (2009) 1601.
[14] A.B. Tamayo, B. Walker, T.Q. Nguyen, J. Phys. Chem. C 112 (2008) 11545.
[15] F. Zhang, J. Bijleveld, E. Perzon, K. Tvingstedt, S. Barrau, O. Inganäs, M.R. Andersson, J. Mater. Chem. 18 (2008) 5468.
[16] H.A. Becerril, N. Miyaki, M.L. Tang, R. Mondal, Y.S. Sun, A.C. Mayer, J.E. Parmer, M.D. McGehee, Z. Bao, J. Mater. Chem. 19 (2009) 591.
[17] W. Mammo, S. Admassie, A. Gadisa, F. Zhang, O. Inganäs, M.R. Andersson, Sol. Energy Mater. Sol. Cells 91 (2007) 1010.
[18] M. Sun, L. Wang, X. Zhu, B. Du, R. Liu, W. Yang, Y. Cao, Sol. Energy Mater. Sol. Cells 91 (2007) 1681.
[19] J. Peet, J.Y. Kim, N.E. Coates, W.L. Ma, D. Moses, A.J. Heeger, G.C. Bazan, Nat. Mater. 6 (2007) 497.
[20] D. Mülhlbacher, M. Scharber, M. Morana, Z. Zhu, D. Waller, R. Gaudiana, C. Brabec, Adv. Mater. 18 (2006) 2884.
[21] Z. Zhu, D. Waller, R. Gaudiana, M. Morana, D. Mülhlbacher, M. Scharber, C. Brabec, Macromolecules 40 (2007) 1981.
[22] H. Sirringhaus, T. Kawase, R.H. Friend, T. Shimoda, M. Inbasekaran, W. Wu, E.P. Woo, Science 290 (2000) 2123.
[23] J. Jo, D. Vak, Y.Y. Noh, S.S. Kim, B. Lim, D.Y. Kim, J. Mater. Chem. 18 (2008) 654.
[24] S. Rait, S. Kashyap, P.K. Bhatnagar, P.C. Mathur, S.K. Sengupta, J. Kumar, Sol. Energy Mater. Sol. Cells 91 (2007) 757.
[25] K.C. Li, Y.C. Hsu, J.T. Lin, C.C. Yang, K.H. Wei, H.C. Lin, J. Polym. Sci. Part A: Polym. Chem. 13 (2008) 4285.
[26] V. Shrotriya, G. Li, Y. Yao, C.W. Chu, Y. Yang, Appl. Phys. Lett. 88 (2006) 073508.
[27] V. Shrotriya, Y. Yao, G. Li, Y. Yang, Appl. Phys. Lett. 89 (2006) 063505.
[28] S. Janietz, D.D.C. Bradley, M. Grelly, C. Giebeler, M. Inbasekaran, E.P. Woo, Appl. Phys. Lett. 73 (1998) 2453.
[29] J.H. Huang, Z.Y. Ho, D. Kekuda, C.W. Chu, K.C. Ho, J. Phys. Chem. C 112 (2008) 19125.
[30] J.H. Huang, C.P. Lee, Z.Y. Ho, D. Kekuda, C.W. Chu, K.C. Ho, Sol. Energy Mater. Sol. Cells (2009). doi:10.1016/j.solmat.2009.02.019.
[31] J.H. Huang, C.Y. Yang, Z.Y. Ho, D. Kekuda, M.C. Wu, F.C. Chien, P. Chen, C.W. Chu, K.C. Ho, Org. Electron. 10 (2009) 27.
[32] J.F. Chang, B. Sun, D.W. Breiby, M.M. Nielsen, T.I. Sölling, M. Giles, I. McCulloch, H. Sirringhaus, Chem. Mater. 16 (2004) 4772.
[33] J.H. Huang, Z.Y. Ho, D. Kekuda, Y. Chang, C.W. Chu, K.C. Ho, Nanotechnology 20 (2009) 025202.
[34] W.D. Gill, J. Appl. Phys. 43 (1972) 5033.
[35] H.Y. Chen, H. Yang, G. Yang, S. Sista, R. Zadoyan, G. Li, Y. Yang, J. Phys. Chem. C 113 (2009) 7946.
[36] J.H. Huang, D. Kekuda, C.W. Chu, K.C. Ho, J. Mater. Chem. 19 (2009) 3704.
[37] C.M. Björström, A. Bernasik, J. Rysz, A. Budkowski, S. Nilsson, M. Svensson, M.R. Andersson, K.O. Magnusson, E. Moons, J. Phys.: Condens. Matter. 17 (2005) L529.
[38] S.Y. Heriot, R.A.L. Jones, Nat. Mater. 4 (2005) 782.